Conrad and Korchynsky parameters cannot be used to interpolate to temperatures other than those actually involved in the stress-rupture testing program; the temperature dependent terms are irrational functions of temperature.

References

[1] Raut, P. K. and Clough, W. R., "Computerized Evaluations of the Relative Abilities of Seven Time-Temperature Parameters to Correlate and Extrapolate Nickel-Alloy Stress-Rupture Data," *Transactions of the ASME: Journal of Basic Engineering*, Ser. D, Vol. 94, March 1972, pp. 7–12.

[2] Larson, F. R. and Miller, J., "A Time-Temperature Relationship for Rupture and Creep Studies," *Transactions of the ASME*, Vol. 74, 1952, pp. 765–777.

[3] Manson, S. S. and Haferd, A. M., "A Linear Time-Temperature Relation for Extrapolation of Creep and Stress-Rupture Data," TN 2894, March 1952, NACA.

[4] Orr, R. L., Sherby, O. D., and Dorn, J. E., "Correlations of Rupture Data for Metals at Elevated Temperatures," *Transactions of the ASME*, Vol. 46, 1954, pp. 113–128.

[5] Manson, S. S. and Succop, G., "Stress-Rupture Properties of Inconel 700 and Correlation on the Basis of Several Time-Temperature Parameters," STP 174, 1956, ASTM, Philadelphia, Pa., pp. 40–46.

[6] Goldhoff, R. M. and Hahn, G. J., "Correlation and Extrapolation of Creep-Rupture Data of Several Steels and Superalloys Using Time-Temperature Parameters," Publication D8-100, 1970, ASM, pp. 199–246.

[7] Conrad, H., "The Correlation of the Stress-Rupture Properties of Nimonic Alloys," *Journal of the Institute of Metals*, Vol. 87, 1958, pp. 347–349.

[8] Conrad, H., "Correlation of High-Temperature Creep and Rupture Data," *Transactions of the ASME: Journal of Basic Engineering*, Ser. D, Vol. 81, 1959, pp. 617–628.

[9] Korchynsky, M., "Faster, Less Expensive Creep-Rupture Data," *Materials in Design Engineering*, Vol. 54, Sept. 1961, pp. 124–126.

[10] Manson, S. S., "Design Considerations for Long-Life at Elevated Temperatures," TP 1-63, 1963, NASA.

[11] Mendelson, A., Roberts, E., Jr., and Manson, S. S., "Optimization of Time-Temperature Parameters for Creep and Stress-Rupture With Applications to Data From German Cooperative Long-Time Creep Program," TN D-2975, 1965, NASA.

[12] Campbell, D. A., "Short-Time Stress-Rupture Properties of Three Steels," TM MT-M21, Sept. 14, 1956, Missile Operation, Chrysler Corp., Detroit, Mich.

[13] Mollica, R. J., "Short-Time Rupture Strength of Cor Ten Steel Under Conditions of Stress Application Prior to Heating," Technical Bulletin B299, Feb. 25, 1958, Missile Div., Chrysler Corp., Detroit, Mich.

[14] Korchynsky, M., "Creep-Rupture Properties of Alloys Near the Melting Point," Rept. to Research Projects Lab., May 28, 1959, The Army Ballistics Missile Agency, Redstone Arsenal, Huntsville, Ala.

[15] Kattus, J. R., "Tensile and Creep Properties of Structural Alloys Under Conditions of Rapid Heating, Rapid Loading, and Short-Times at Temperatures," April 10, 1959, Southern Research Institute Report to the International Nickel Co. Inc., New York.

[16] Smith, G. A., "Stress-Rupture Data for AISI 304, AISI 321, and Armco 17-7 PH Stainless Steels," TM MT-M34, April 22, 1957, Missile Div., Chrysler Corp., Detroit, Mich.

[17] Lundin, C. D., Aronson, A. H., Jackman, L. A., and Clough, W. R., "Very-Short-Time, Very-High-Temperature Creep-Rupture of Type 347 Stainless Steel and Correlation of Data," *Transactions of the ASME: Journal of Basic Engineering*, Ser. D, Vol. 91, 1969, pp. 32–38.

[18] Eriksson, J. K. and Clough, W. R., "The Dynamic Creep-Rupture of an 18-18-2 Stainless Steel," *Seventh International Symposium on High-Speed Testing: The Rheology of Solids*, Wiley, New York, 1969, pp. 181–197.

[19] Bernett, E. C., "Short-Time Tensile Creep Properties of 17-7PH Stainless Steel Sheet," Lab. Rept. MP-60, Aug. 5, 1959, Materials and Processes Lab., Marquardt Corp., Van Nuys, Calif.

[20] Bernett, E. C., "Tenile and Short-Time Creep Properties of N155 Alloy Sheet," *Transactions of the ASME: Journal of Engineering for Industry*, Ser. C, Vol. 82, 1960, pp. 283–302.

[21] von Bandel, G. and Gravenhorst, H., "Behavior of High Temperature Steels During Creep Testing at Temperatures of 500 to 700°C," *Archiv fur des Eisenhuttenwesen*, Vol. 28, May–June, 1957, pp. 253–270.

NOVEMBER 1972 J. SPACECRAFT VOL. 9, NO. 11

A Practical Approach to Spacecraft Structural Dynamics Problems

M. R. TRUBERT*
Jet Propulsion Laboratory, Pasadena, Calif.

This paper is concerned with the system approach for structural dynamics. First, the concept of dynamic mass is presented. Second, the determination of a dynamic mass is given relative to the reaction forces and moments between two substructures in terms of the cantilever normal modes of one substructure. Third, it is shown how one can simply couple and uncouple substructures for dynamics problems. Fourth, an example is given for the digital simulation of a sine wave test for the purpose of calculating rotational response of the shaker. Fifth, forcing functions are mathematically determined from the measured responses of the space vehicle in flight. Finally, it is shown how one can perform a hybrid test simulation by combining a real-time analog computer with digitally determined structural characteristics, shaker properties and actual control equipment in order to investigate the stability of the control loop.

Received March 30, 1972; presented as Paper 72-349 at the AIAA/ASME/SAE, 13th Structures, Structural Dynamics, and Materials Conference, San Antonio, Texas, April 10–12, 1972; revision received July 5, 1972. This paper presents the results of one phase of research carried out at the Jet Propulsion Laboratory, California Institute of Technology, under Contract NAS 7-100, sponsored by NASA.

Index categories: Launch Vehicle and Missile Structural Design; Launch Vehicle or Missile System and Component Ground Testing; Unmanned Lunar and Interplanetary System.

* Group Supervisor, Applied Mechanics Division. Member AIAA.

Introduction

BUILDING from the classical normal mode analysis,[1–5] the structural analysis techniques have evolved in several directions in the recent past. The system approach, borrowing from the ideas of electrical engineering, has been introduced in Ref. 6, which has permitted the analytic coupling of substructure analysed at separate times or by separate organizations, as is the case for most aerospace structures. Viewed from a different angle, the system approach has brought the frequency domain into structural dynamics.[7–12] Then, the

advent of the fast Fourier transform algorithm[13] has allowed an economical computer use of the frequency domains approach and has led to the development of computer programs such as those of Ref. 14.

In this paper it will be shown that by proper arrangement of the structural parameters one can introduce the concept of a dynamic mass of a structure in the frequency domain, which has a striking similarity with Newton's law. This concept has the advantage of giving the engineer a physical feel for the problem he has to solve. It will then be shown how the component mode approach and the frequency domain approach can be combined in a practical application.

Very recently, the frequency domain approach has been used at JPL to solve the problem of determining the load on a space structure from the response measured during actual flights.[15,16] This load can then be used as an input to predict the response of future spacecraft.[17]

Finally, a unique combination of digital analysis and analog simulation coupled with actual electronic control hardware will be presented to show how one can use tools of different fields to solve practical dynamics problems.

Newton's Law in the Frequency Domain for a Linear Multi degree-of-Freedom System

In this section, we will be concerned with the idea of "dynamic" mass for a linear elastic structure subjected to dynamic loads. Our approach may appear academic at this point, but it is only intended to illustrate a fundamental idea. A more practical viewpoint will be taken later in a specific application. The equations of motion of a discretized elastic system, assuming viscous damping, are

$$[M]\{\ddot{x}\} + [C]\{\dot{x}\} + [K]\{x\} = \{f\} \tag{1}$$

where $[M]$ is the $n \times n$ mass matrix; $[C]$ is the $n \times n$ damping matrix; $[K]$ is the $n \times n$ stiffness matrix; $\{x\} = \{x(t)\}$ is the column of the degrees of freedom; $\{f\} = \{f(t)\}$ is the column of the loads.

Let us take the Fourier transform of both sides of Eq. (1). By convention, a bar over a variable means Fourier transform. For example,

$$\{\bar{a}_x\} = \int_{-\infty}^{+\infty} \{\ddot{x}(t)\} e^{-i\omega t} dt \tag{2}$$

where ω is the circular frequency in rad/sec. Then, Eq. (1) becomes

$$[M + C/i\omega - k/\omega^2]\{\bar{a}_x\} = \{\bar{f}\} \tag{3}$$

The matrix premultiplying $\{\bar{a}_x\}$ is a frequency-dependent matrix which we will call the dynamic mass and which is a generalization of the mass and inertia of a rigid body. Let

$$[M + C/i\omega - K/\omega^2] = [\mathscr{M}(\omega)] = [\mathscr{M}] \tag{4}$$

Equation (3) can then be rewritten as

$$\{\bar{f}\} = [\mathscr{M}]\{\bar{a}_x\} \tag{5}$$

which appears as a generalization of Newton's law in the frequency domain in a multidimensional space; i.e., force is equal to mass times acceleration. The size of matrix $[\mathscr{M}]$ is, in general, very large (several hundred or even several thousand); consequently, using Eq. (5) to solve for the response would be impractical. As a result, in order to reduce the size of the problem a normal mode analysis is usually sought from Eq. (1). The type of modes to be considered varies with the problem at hand, and a general expression of $[\mathscr{M}]$ in terms of the normal modes is not very meaningful and will not be given here.

Reaction Forces and Moments at the Interface of Two Substructures

Let us assume that a flexible substructure S_1 (Fig. 1), e.g., a spacecraft under laboratory dynamic test, is attached to another substructure S, e.g., a shaker head. We will assume at this time, for simplicity, that the plane of the interface is so rigid that it remains plane during the motion of the whole system. The objectives are to determine the reaction forces and moments at the interface. The dynamic characteristics of the structure S_1 are most conveniently introduced by the normal modes in a configuration cantilevered at the interface. Let us assume that a classical normal mode analysis has been performed and that N normal modes have been retained. The Eqs. of motion of the structure S_1 in an imposed base motion are[6]

$$\left[\begin{array}{c|c} M_{RR} & M_{ER} \\ \hline M_{RE} & M_{EE} \end{array}\right] \begin{Bmatrix} \ddot{R} \\ \hline \ddot{q} \end{Bmatrix} + \left[\begin{array}{c|c} 0 & 0 \\ \hline 0 & C_{EE} \end{array}\right] \begin{Bmatrix} \dot{R} \\ \hline \dot{q} \end{Bmatrix} + \left[\begin{array}{c|c} 0 & 0 \\ \hline 0 & K_{EE} \end{array}\right] \begin{Bmatrix} R \\ \hline q \end{Bmatrix} = \begin{Bmatrix} f \\ \hline 0 \end{Bmatrix} \tag{6}$$

where $[M_{RR}]$ is the rigid body mass matrix (6×6) of the spacecraft with respect to its base; $[M_{EE}]$ is the generalized mass matrix ($N \times N$); $[M_{RE}] = [M_{ER}]^T$ is the rigid-elastic coupling term matrix ($N \times 6$); $[C_{EE}]$ is the damping matrix ($N \times N$); $[K_{EE}]$ is the generalized stiffness matrix ($N \times N$); $\{R\}$ is the column of the base motion (6×1); $\{q\}$ is the modal response with respect to the base ($N \times 1$); $\{f\}$ is the column of the reaction forces and moments (6×1).

Taking the Fourier transform of both sides of Eq. (6) and separating the equations, we have

$$[M_{RR}]\{\bar{a}_R\} + [M_{ER}]\{\bar{a}_q\} = \{\bar{f}\} \tag{7}$$

$$[M_{RE}]\{\bar{a}_R\} + [Z]\{\bar{a}_q\} = 0 \tag{8}$$

with

$$[Z(\omega)] = [Z] = [M_{EE}] - (1/\omega^2)[K_{EE}] - (i/\omega)[C_{EE}] \tag{9}$$

Since $[Z]$ is a diagonal matrix, it can easily be inverted, and we can solve Eq. (8) for $\{\bar{a}_q\}$ and substitute into Eq. (7). After reduction, we obtain

$$[M_{RR} - M_{ER}Z(\omega)^{-1}M_{RE}]\{\bar{a}_R\} = \{\bar{f}\} \tag{10}$$

The matrix premultiplying $\{\bar{a}_R\}$, i.e.,

$$[\mathscr{M}(\omega)] = [M_{RR} - M_{ER}Z(\omega)^{-1}M_{RE}] \tag{11}$$

is the dynamic mass of S_1 viewed from the reaction forces and moments applied at the base of the spacecraft. The dynamic mass matrix $[\mathscr{M}(\omega)]$ is a combination of the real mass (and inertia) matrix $[M_{RR}]$ and a frequency-dependent matrix expressed in terms of the rigid-elastic coupling matrices. In conclusion, the reaction forces and moments are obtained from Eq. (10) by writing Newton's law between the reaction forces $\{\bar{f}\}$, the base acceleration $\{\bar{a}_R\}$ and the dynamic mass $[\mathscr{M}(\omega)]$

$$\{\bar{f}\} = [\mathscr{M}(\omega)]\{\bar{a}_R\} \tag{12}$$

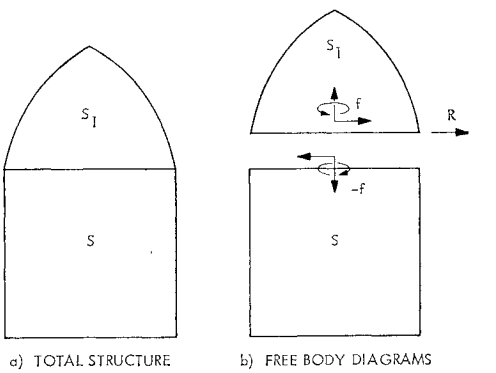

Fig. 1 Substructures S and S_1 with statically determinate interface.

Coupling and Uncoupling of Structures

A first structure Σ_1 is made of a main structure S and substructure S_1 (Fig. 2). The main structure S and the substructure S_1 are connected at N points $A_1, A_2, \ldots, A_N$. We call $\{u_1{}^1\}, \{u_2{}^1\}, \ldots, \{u_N{}^1\}$ the time variable motions of the interface points $A_1, A_2, \ldots, A_N$ with respect to a given inertial frame of reference. Each of the points may have between 1 and 6 degrees of freedom, depending upon the type of connection used. We call $\{u^1\}$ the column formed by all the degrees of freedom of $A_1, A_2, \ldots, A_N$

$$\{u^1\} = \begin{Bmatrix} u_1{}^1 \\ \hline u_2{}^1 \\ \hline \vdots \\ \hline u_N{}^1 \end{Bmatrix} = \begin{Bmatrix} u_1{}^1 \\ \vdots \\ u_M{}^1 \end{Bmatrix} \quad M \leq 6N \tag{13}$$

Time variable forces and moments, which we will call forcing function, $\{F_1\}, \{F_2\}, \ldots, \{F_p\}$ are applied at points $P_1, P_2, \ldots, P_p$ of structure S. Each column $\{F_j\}$ has one to three components of forces and moments. We call $\{F\}$ the column for the total number of components of forces and moments

$$\{F\} = \begin{Bmatrix} F_1 \\ \hline F_2 \\ \hline \vdots \\ \hline F_p \end{Bmatrix} = \begin{Bmatrix} F_1 \\ \vdots \\ F_Q \end{Bmatrix}, \quad Q \leq 6p \tag{14}$$

Here again, there exists a dynamic mass matrix $[\mathcal{M}_1(\omega)]$ between $\{\bar{F}\}$ and the acceleration $\{\bar{a}_u{}^1\}$. This matrix $[\mathcal{M}_1(\omega)]$ can be obtained either by a modal analysis or by actual modal test measurements or a combination of both. In any case, we have

$$\{\bar{F}\} = [\mathcal{M}_1(\omega)]\{\bar{a}_u{}^1\} \tag{15}$$

An expression of $[\mathcal{M}_1(\omega)]$ is shown in the appendix.

Let us assume now that the substructure S_1 is removed and replaced by a new known substructure S_2. The objective is to determine the dynamic mass matrix $[\mathcal{M}_2(\omega)]$ relating the forcing function $\{\bar{F}\}$ and the new motion $\{\bar{a}_u{}^2\}$ at the interface points $A_1, A_2, \ldots, A_N$

$$\{\bar{F}\} = [\mathcal{M}_2(\omega)]\{\bar{a}_u{}^2\} \tag{16}$$

Let us make a cut through the points $A_1, A_2, \ldots, A_N$ for the first structure Σ_1; reaction forces and moments $\{f^1\}$ are present in S_1 and S to satisfy the equilibrium. Call $[S_1(\omega)]$ the dynamic mass matrix of the substructure S_1 relating the acceleration $\{\bar{a}_u{}^1\}$ to the reaction forces and moments $\{\bar{f}^1\}$. Newton's law in the frequency domain gives

$$\{\bar{f}^1\} = [S_1(\omega)]\{\bar{a}_u{}^1\} \tag{17}$$

The dynamic mass matrix $[S_1(\omega)]$ is obtained from the cantilevered modes using Eq. (11), where $[\mathcal{M}(\omega)]$ is replaced by $[S_1(\omega)]$.

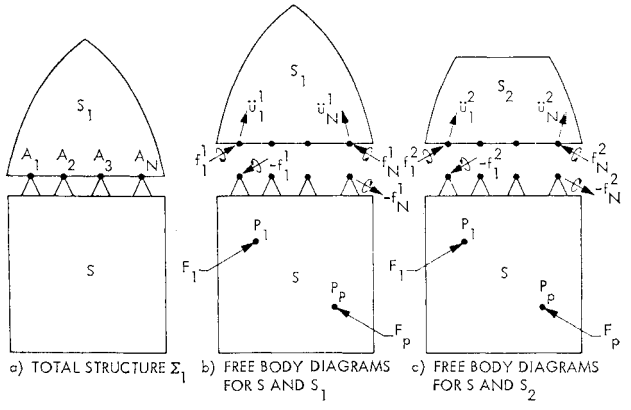

Fig. 2 Coupling and uncoupling of substructures.

Call $[S(\omega)]$ the dynamic mass matrix of the main structure alone, relating the motion $\{\bar{a}_u{}^1\}$ to the forces and moments $\{-\bar{f}^1\}$ and $\{\bar{F}\}$

$$\{-\bar{f}^1\} + \{\bar{F}\} = [S(\omega)]\{\bar{a}_u{}^1\} \tag{18}$$

Combining Eqs. (17) and (18), we obtain

$$\{\bar{F}\} = [S_1(\omega) + S(\omega)]\{\bar{a}_u{}^1\} \tag{19}$$

Comparing Eqs. (15) and (19) shows that the dynamic mass matrix $[\mathcal{M}_1(\omega)]$ is

$$[\mathcal{M}_1(\omega)] = [S_1(\omega) + S(\omega)] \tag{20}$$

A similar relationship exists when the substructure S_1 is replaced by another substructure S_2

$$[\mathcal{M}_2(\omega)] = [S_2(\omega) + S(\omega)] \tag{21}$$

where $[S_2(\omega)]$ is the dynamic mass matrix relating the acceleration $\{\bar{a}_u{}^2\}$ to the reaction forces and moments $\{\bar{f}^2\}$ at the base of the substructure S_2.

Combining Eqs. (20) and (21), we obtain the new dynamic mass matrix

$$[\mathcal{M}_2(\omega)] = [\mathcal{M}_1(\omega) - S_1(\omega) + S_2(\omega)] \tag{22}$$

The new mass matrix $[\mathcal{M}_2(\omega)]$ for the combination S and S_2 is obtained by subtracting the mass matrix of the substructure $[S_1(\omega)]$ and adding the mass matrix $[S_2(\omega)]$ of the substructure S_2 to the original mass matrix $[\mathcal{M}_1(\omega)]$.

Spacecraft Environmental Vibration Test Simulation

Environmental sinusoidal forced vibration tests are performed on spacecraft prior to launch in order to verify the ability of the structure to survive the dynamic environment induced by the launch vehicle. Those tests are implemented by mounting the whole spacecraft on the moving armature of a large electrodynamic shaker. The objective of the test is to reproduce an environment at the base of the spacecraft which excites the structure to a level enveloping the actual launch environment. The Mariner Mars 1971 spacecraft, designed and built at JPL, presented a fair amount of dissymmetry, mainly due to the weight difference between the two large tanks of the propulsion subsystem to be used at Mars encounter in placing the spacecraft in orbit around the planet. As a result of this dissymmetry, it was anticipated that an overturning moment of substantial magnitude at the base of the spacecraft could possibly occur during the environmental sinusoidal vibration test at certain resonant frequencies. A large overturning moment would have presented potential damaging effects on the armature of the shaker by creating large lateral and rotational armature displacements and possibly subsequent damage to the spacecraft. Therefore, a detailed dynamic analysis was made to calculate the armature displacements during a computer simulation of the vibration test.

The dynamic characteristics of the shaker and the spacecraft had to be known in order to carry out this analysis and simulation. The method outlined in the previous section was implemented. A combination of modal test and analysis was employed to obtain the models. Knowing the dynamic characteristics of the shaker armature was of primary importance, since it was in essence the support structure for the whole spacecraft in the testing configuration. It was believed that dynamic modal tests rather than static tests would be preferable to obtain those dynamic characteristics. To this end, a rigid mass of about 500 kg was mounted on the shaker armature, and eight natural frequencies, mode shapes, and dampings were determined experimentally.

The details of the modal test can be found in Ref. 18. The dynamic characteristics of the Mariner Mars 1971 spacecraft without the solar panels were also determined by a separate

modal test made on the spacecraft cantilevered on the floor.[18] Seven measured natural modes were retained, to which four slosh modes and four solar panel modes were mathematically added,[6] to form a 15 normal-mode model of the spacecraft.

Referring to the previous section, the main structure S is the shaker, the substructure S_1 is the rigid mass, and the substructure S_2 is the Mariner Mars 1971 spacecraft. The dynamic mass matrix $[\mathscr{M}_1(\omega)]$ in terms of the measured normal modes of the shaker loaded by the rigid mass is, according to the Appendix,

$$[\mathscr{M}_1(\omega)] = [V_u\, Y(\omega) V_F{}^T]^{-1} \tag{23}$$

The dynamic mass matrix $[S_2(\omega)]$ has the same form as Eq. (11), since the modal test was performed on the spacecraft cantilevered at its base on the floor, and the interface between shaker armature and spacecraft is assumed to be statically determinate

$$[S_2(\omega)] = [M_{RR} - M_{ER} Z(\omega)^{-1} M_{RE}] \tag{24}$$

The dynamic mass matrix $[S_1(\omega)]$ is simply the mass, static unbalance and inertia matrix $[M_0]$, since the structure S_1 is a rigid mass

$$[S_1(\omega)] = [M_0] \tag{25}$$

Finally, the dynamic mass matrix $[\mathscr{M}_2(\omega)]$ of the spacecraft/shaker combination is

$$[\mathscr{M}_2(\omega)] = [[V_u Y(\omega) V_F{}^T]^{-1} - M_0 + M_{RR} - M_{ER} Z(\omega)^{-1} M_{RE}] \tag{26}$$

This matrix was computed numerically on a digital time share computer for given ranges of frequencies.

The forcing function is a simple vertical sinusoidal force

$$F = F_0 \sin\omega t \tag{27}$$

so that the column $\{\bar{F}\}$ has only one nonzero term

$$\{\bar{F}\} = \begin{Bmatrix} 0 \\ 0 \\ 0 \\ F_0 \\ 0 \\ 0 \end{Bmatrix} = \begin{Bmatrix} 0 \\ \hline F_0 \end{Bmatrix} \tag{28}$$

As is usually the case for environmental testing, the test is electronically controlled such that the acceleration in one direction at the base of the spacecraft (here the vertical acceleration $\ddot{z}_0$) is maintained at a given constant level for a given frequency range. Here again, the frequency domain as used so far is very appropriate to solve for the response of the base of the spacecraft in terms of a known acceleration $\bar{a}_z$. The dynamic mass matrix $[\mathscr{M}_2)\omega)]$ of the shaker/spacecraft/combination is partitioned to correspond to the partition shown in Eq. (28). To avoid inconvenient subscripts, the matrix $[\mathscr{M}_2(\omega)]$ is renamed $[H(\omega)]$

$$[\mathscr{M}_2(\omega)] \equiv [H(\omega)] \tag{29}$$

Equation (16) then becomes, after partitioning

$$\begin{Bmatrix} 0 \\ \hline F_0 \end{Bmatrix} = \left[\begin{array}{c|c} H_1 & H_2 \\ \hline H_3 & H_4 \end{array}\right] \begin{Bmatrix} \bar{a}_r \\ \hline \bar{a}_z \end{Bmatrix} \tag{30}$$

where the acceleration $\{\bar{a}_u{}^2\}$ at the top of the armature has been partitioned as follows

$$\{\bar{a}_u{}^2\} = \begin{Bmatrix} \bar{a}_r \\ \hline \bar{a}_z \end{Bmatrix} \tag{31}$$

The column $\{\bar{a}_r\}$ represents the two lateral accelerations and the three rotations of the top of the shaker armature. This column can easily be obtained from Eq. (30)

$$\{\bar{a}_r\} = -[H_1]^{-1}[H_2]\bar{a}_z \tag{32}$$

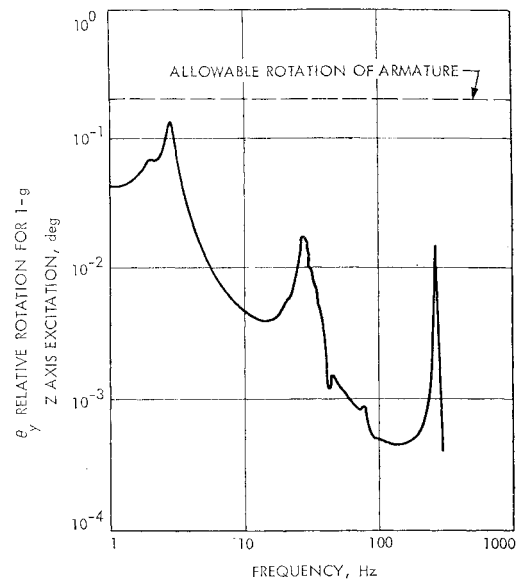

Fig. 3 Armature rotation for spacecraft vibration test.

The relative motion of the armature with respect to the shaker body can be obtained by introducing the stiffness of the flexure connecting shaker body with armature or by computing the motion of the shaker body and subtracting it from Eq. (32).[18] A typical plot of the relative rotational acceleration of the armature is shown in Fig. 3. This simulation showed that the armature rotation was below the allowable limit and that the lateral motion was negligible.

Determination of Loads From Flight Data

Determining flight loads on a spacecraft during the boost phase has always been at best a difficult problem because only a limited number of flights exist and all data have to be transmitted to ground via telemetry. For these reasons, only a limited amount of data is available, and a special effort is required to make best use of these data. The easiest structural data that can be obtained are accelerations at selected locations of the space vehicle, provided enough telemetry channels are open to the structural engineer. The opportunity to record acceleration flight data of a sufficient amount was given to the structure engineers during the flight of six Atlas/Centaur launch vehicles carrying the Mariner Mars 1969, Orbiting Astronomical Observatory (OAO), and Applications Technology Satellite (ATS) spacecraft.

Six components of acceleration at the base of the spacecraft were recorded during the boost phase. Assuming that the base of the spacecraft is sufficiently rigid to move as a plane, those six components completely determine the motion of the base of the spacecraft. In addition, some of the events which take place during the boost phase, such as the Centaur engine shutdown, have an origin sufficiently well located so that is is possible to work "backward" from the response to determine the magnitude of the transient dynamic load which occurs at this event. The analytical method to be followed is fully described in Refs. 15 and 17 and has been successfully applied to several spacecraft.

The problem is unusual in the sense that the response is the known quantity while the load is the unknown quantity. A first attempt to solve the problem in the time domain was unsuccessful,[19] because of the existence of complex eigenvalues with positive real parts. The existence of such eigenvalues is due to the nature of the "inverse" solution. It was found that the frequency domain solution circumvents this difficulty.

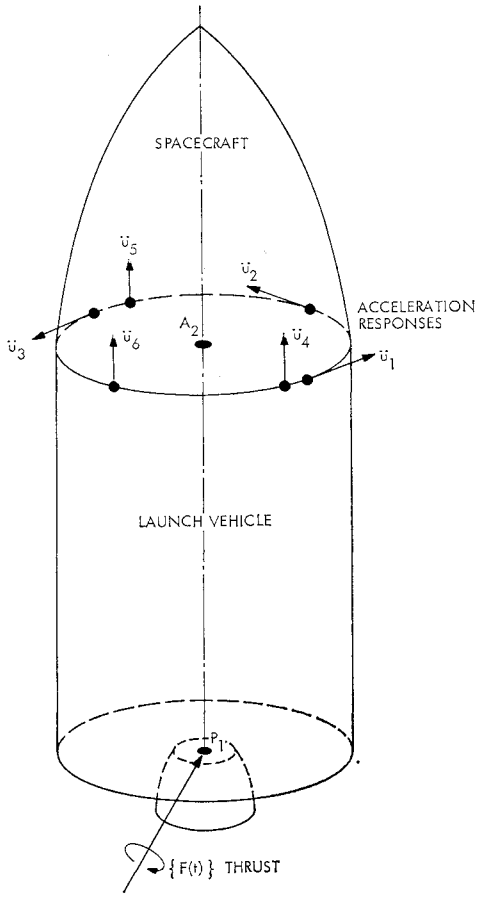

Fig. 4 Launch vehicle and spacecraft.

Figure 4 represents a typical launch vehicle carrying a spacecraft. The accelerations $\ddot{u}_1(t), \ddot{u}_2(t), \ldots, \ddot{u}_6(t)$ are the six accelerations telemetered to ground. They are at the plane of the interface between the launch vehicle and the spacecraft. A transient forcing function (the thrust) $\{F(t)\}$ having six components (three forces and three moments) $F_1(t), F_2(t), \ldots, F_6(t)$ exists at the base of the launch vehicle at Centaur engine shutdown. The problem is to determine $\{F(t)\}$ from $\{\ddot{u}(t)\}$. A good mathematical model of the composite vehicle made of the launch vehicle and the spacecraft has first to be derived in order to carry out the solution.

Here again, there exists a dynamic mass matrix $[\mathcal{M}(\omega)]$ between the Fourier transform of the thrust $\{\bar{F}\}$ and the Fourier transform of the response $\{\bar{a}_u\}$

$$\{\bar{F}\} = [\mathcal{M}(\omega)]\{\bar{a}_u\} \tag{33}$$

The mathematical derivation of $[\mathcal{M}(\omega)]$ is given in Ref. 15 as

$$[\mathcal{M}(\omega)] = [\phi_{2r}M_{rr}^{-1}\phi_{1r} + \phi_{2e}Z(\omega)^{-1}\phi_{1e}]^{-1} \tag{34}$$

which is a rewriting of Eq. (A12) of the Appendix with the addition of the rigid body modes, since the composite vehicle is in a free boundary condition.

In Eq. (34), $[\phi_{1r}]$, $[\phi_{2r}]$ are the matrices of the rigid body modes shapes at points P_1 and A_2, respectively; $[\phi_{1e}]$, $[\phi_{2e}]$ are the matrices of the elastic mode shapes at points P_1 and A_2, respectively; $[M_{rr}]$ is the rigid body mass matrix of the composite vehicle with respect to point P_1; $[Z(\omega)]^{-1} = [Y]$ is the matrix shown in Eq. (A6). Computer programs which performed all the necessary calculations are indicated in Ref. 16.

Figures 5 and 6 show the time histories and Fourier transform of a "typical" component of the response and the forcing function determined by the inverse solution for Mariner Mars 1971 and Viking spacecraft. Six such components exist for P_1 and A_2 (Ref. 17).

Once the forcing function $\{F(t)\}$ is known, it can be used as a known load to predict the response of a new spacecraft to be flown on a launch vehicle of the same type (here, the Centaur). Models corresponding to the new spacecraft are, of course, needed.

Statistical calculation on the response would be desirable; however, the number of sample flights being small, the statistical properties of the ensemble remain unknown. One can only predict how the new spacecraft would have responded if it had been flown on the launch vehicle used with a previous spacecraft. This limited prediction information is nevertheless very valuable to the designer.

Real-Time Analog Simulation of the Control/Shaker/Spacecraft Interaction for a Forced Vibration Test

In this section, we will deal with the simulation of a forced vibration test using a technique which combines the analytical model of a structure under test determined by digital means, a real-time analog representation of the structure and shaker, and the actual control equipment.

Test implementation difficulties encountered during forced vibration testing of the Mariner Mars 1971 propulsion subsystem resulted in a study for the evaluation of the capability of the acceleration control system used during the test. One phase of this evaluation was accomplished with the aid of an

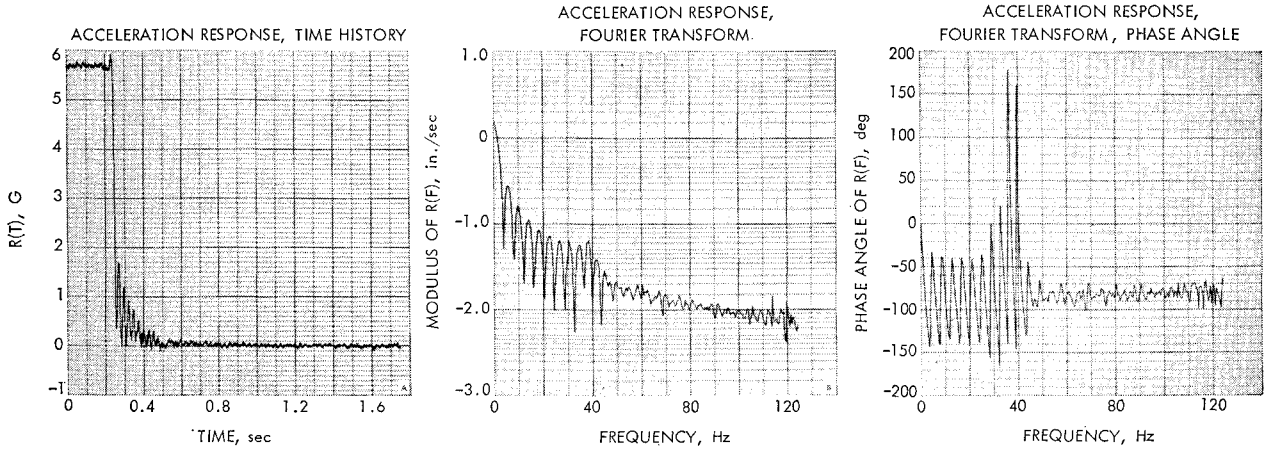

Fig. 5 Component of typical flight response.

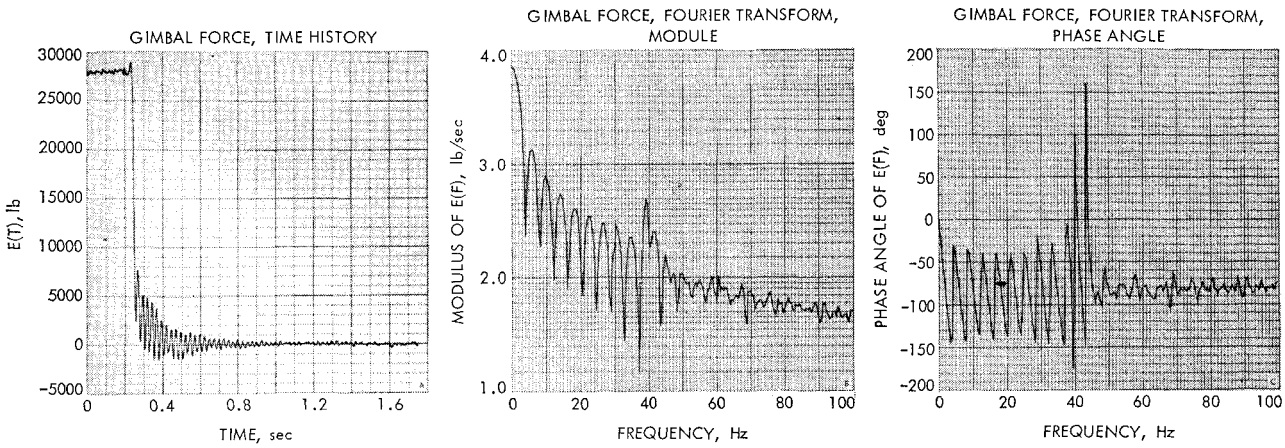

Fig. 6 Component of typical forcing function.

analog computer which simulated the dynamic characteristics of the propulsion subsystem, the vibration exciter, and amplifier electrical characteristics. The acceleration control equipment was connected directly to the analog simulation as shown in Fig. 7, using the actual sweep oscillator and servo-control system. This configuration of analog simulation of the structure and vibration exciter and test control equipment provided the capability of varying test parameters such as structural damping, structural shaker frequencies, sweep rate, compressor speeds, and others in evaluating the effects of parametric changes on the control unit in real-time.

The mathematical model used to represent the propulsion subsystem was a spring mass idealization whose dynamic characteristics were represented by 12 modes of an eigenvalue solution obtained from digital computer analysis. The dynamic characteristics of the vibration exciter, the armature flexures and trunnions, were obtained from the results of a modal test accomplished on the vibration exciter loaded with a rigid 700 kg mass of known inertial properties. The two separate models were then mathematically combined using a modified modal combination technique[18] and truncated to six modes each giving a mathematical representation of the propulsion subsystem in the frequency range of 10 to 50 Hz. The resulting model and the electrical characteristics of the vibration exciter were simulated on a real-time analog computer as shown in Fig. 7.

The eight control accelerometers located in a horizontal plane at the interface of the propulsion subsystem and the test fixture and the two response transducers on the propellant

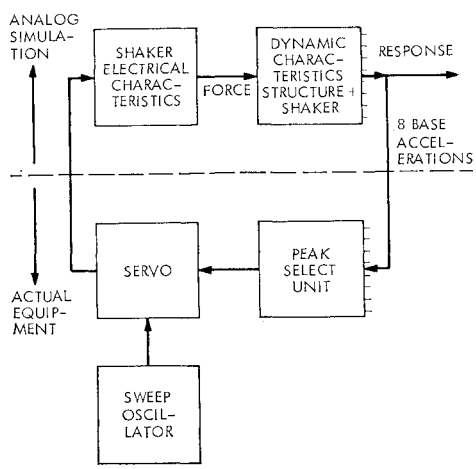

Fig. 7 Analog simulation/control hardware layout for forced vibration test simulation.

tanks were simulated by the analog and connected to the control unit (Fig. 7). The control loop was closed through the servo to the input of the real-time analog computer. The whole system was driven by a sinewave sweep oscillator.

A large number of simulation runs were accomplished from 10 to 80 Hz. Several settings of the control unit were tried for these runs. A parametric study of the influence of the modal damping on the structural response was conducted by arbitrarily decreasing or increasing the damping of each mode of the spacecraft model and the shaker model. In addition, a limited number of runs were made with some degree of nonlinearities for both damping and natural frequencies of some critical modes of the spacecraft and the shaker. Although the exact test difficulties of the real test were not completely simulated, the similarity of control behavior, more specifically, the rate of change of correction (compressor speed), was sufficient to evaluate and demonstrate that the control system as used for the original test was marginally adequate to satisfy the objectives of the intended test program. Such a study was very helpful in determining a new test procedure for the subsequent environmental vibration tests.

Conclusion

To conclude, it can be said that the frequency domain approach and the analog simulation in combination with the classical eigenvalue solution of structural problems can play a very useful role in structural dynamics.

Appendix: Dynamic Mass Matrix in Terms of the Normal Modes

Let us assume that the normal modes of a structure are known either by numerical analysis or by modal test. Assuming modal damping, the response $\{\ddot{u}\}$ due to a forcing function $\{F\}$ is given by the following matrix equation[4]

$$[\mu_i]\{\ddot{q}\} + [\beta_i]\{\dot{q}\} + [\gamma_i]\{q\} = [V]^T\{F\} \tag{A1}$$

$$\{\ddot{u}\} = [V]\{\ddot{q}\} \tag{A2}$$

where $[\gamma_i]$, $[\beta_i]$, $[\gamma_i]$ are the generalized mass, generalized damping, and generalized stiffness matrices, $[V]$ is the modal matrix and $\{q\}$ are the generalized coordinates.

Working in the frequency domain allows an easy solution of these equations by transforming differential equations into algebraic equations.

After taking the Fourier transform of these equations, we obtain

$$[\mu - (i/\omega)\beta - \gamma/\omega^2]\{\bar{a}_q\} = [V]^T\{\bar{F}\} \quad \text{(A3)}$$

$$\{\bar{a}_u\} = [V]\{\bar{a}_q\} \quad \text{(A4)}$$

Solving Eq. (A3) for $\{\bar{a}_q\}$ and substituting into Eq. (A4), we obtain

$$\{\bar{a}_u\} = [VY(\omega)V^T]\{\bar{F}\} \quad \text{(A5)}$$

where the diagonal matrix $[Y(\omega)]$ is

$$[Y(\omega)] = [\mu - (i/\omega)\beta - \gamma/\omega^2]^{-1} \quad \text{(A6)}$$

Calling μ_n the generalized mass of each mode ($n = 1, 2, \ldots, N$), we find that the corresponding generalized damping and stiffness of each mode is

$$\beta_n = 2\mu_n\xi_n\omega_n \quad \text{(A7)}$$

$$\gamma_n = \mu_n\omega_n^2 \quad \text{(A8)}$$

where ξ_n and ω_n are the modal dampings and the natural frequencies. Therefore, each term Y_n of the matrix $[Y(\omega)]$ is

$$Y_n = \frac{\omega^2}{\mu_n(\omega^2 - \omega_n^2 - 2i\xi_n\omega\omega_n)}$$

Solving Eq. (A5) for $\{\bar{F}\}$ gives

$$\{\bar{F}\} = [VY(\omega)V^T]^{-1}\{\bar{a}_u\} \quad \text{(A10)}$$

The matrix premultiplying $\{\bar{a}_u\}$ is the dynamic mass matrix.

In practice, it is not necessary to consider the complete modal matrix $[V]$ but only the one which corresponds to the mode shapes $[V_F]$ where the forces are applied and the mode shapes $[V_u]$ where the responses are measured. However, the number of forces and the number of responses must be equal to make the matrix $[V_uY(\omega)V_F^T]$ a square matrix in order to perform inversion. If the number of forces is not equal to the number of responses, zero will be added to either column $\{\bar{F}\}$ or $\{\bar{a}_u\}$ with corresponding actual modal terms in $[V_F]$ of $[V_u]$. We will have

$$\{\bar{F}\} = [V_uY(\omega)V_F^T]^{-1}\{\bar{a}_u\} \quad \text{(A11)}$$

The dynamic mass is

$$[\mathcal{M}(\omega)] = [V_uY(\omega)V_F^T]^{-1} \quad \text{(A12)}$$

References

[1] Scanlan, R. H. and Rosenbaum, R., *Introduction to the Study of Aircraft Vibration and Flutter*, Macmillan, New York, 1951.

[2] Bisplinghoff, R. L., Ashley, H., and Halfman, R. L., *Aeroelasticity*, Addison-Wesley, Reading, Mass., 1955.

[3] Myklestad, N. O., *Fundamentals of Vibration Analysis*, McGraw-Hill, New York, 1956.

[4] Hurty, W. C. and Rubinstein, M. F., *Dynamics of Structures*, Prentice-Hall, Englewood Cliffs, N. J., 1964.

[5] Pestel, C. E. and Leckie, F. A., *Matrix Methods in Elasto Mechanics*, McGraw-Hill, New York, 1963.

[6] Hurty, W. C., "Dynamics Analysis of Structural Systems Using Component Modes," *AIAA Journal*, Vol. 3, No. 4, April 1965, p. 678.

[7] Hixon, L. E., "Mechanical Impedance and Mobility," *Shock and Vibration Handbook*, Vol. 1, McGraw-Hill, New York, 1961, p. 10–1.

[8] Trubert, M. R., "Response of Elastic Structures to Statically Correlated Multiple Random Vibration," *Journal of the Acoustical Society of America*, Vol. 35, 1963.

[9] Rubin, S., "Mechanical Immittance and Transmission Matrix Concept," *Journal of the Acoustical Society of America*, Vol. 41, May 1967.

[10] O'Hara, G. J., "Mechanical Impedance and Mobility Concepts," *Journal of the Acoustical Society of America*, Vol. 41, May 1967.

[11] Trubert, M., "Structural and Electromechanical Interaction in the Multiple Exciter Technique for Random Vibration Testing," *Journal of the Acoustical Society of America*, Vol. 41, May 1967.

[12] Heer, E. and Trubert, M. R., "Analysis of Space Vehicle Structures Using the Transfer Function Concept," *Proceedings of the 19th International Astronautical Congress, New York 1968*, Vol. 1, Pergamon Press, New York, 1970.

[13] Cooley, J. W. and Tukey, T. W., "An Algorithm for the Machine Calculation of Complex Fourier Series," *Mathematics of Computation*, Vol. 19, 1965, pp. 297–301.

[14] Simpson, R. and Kruck, R., "Receptance Coupling Program," Rept. 900-442, March 31, 1971, Jet Propulsion Lab., Pasadena, Calif.

[15] Trubert, M. R., Chisholm, J. R., and Gayman, W. H., *Use of Centaur/Spacecraft Flight Data in the Synthesis of Forcing Functions at Centaur Main Engine Cutoff During Boost of Mariner Mars 1969, OAO-II, and ATS Spacecraft: Analysis and Evaluation*, TM 33-487, Vol. I, June 21, 1971, Jet Propulsion Lab., Pasadena, Calif.

[16] Trubert, M. R., Chisholm, J. R., and Gayman, W. H., *Use of Centaur/Spacecraft Flight Data in the Synthesis of Forcing Functions at Centeur Main Engine Cutoff During Boost of Mariner Mars 1969, OAO-II, and ATS Spacecraft: Computer Plots*, TM 33-487, Vol. II, June 21, 1971, Jet Propulsion Lab., Pasadena, Calif.

[17] Trubert, M. R., Chisholm, J. R., and Gayman, W. H., *Use of Derived Forcing Functions at Centaur Main Engine Cutoff in Predicting Transient Loads on Mariner Mars 1971 and Viking Spacecraft*, TM 33-486, June 28, 1971, Jet Propulsion Lab., Pasadena, Calif.

[18] Freeland, R. E., *Mariner Mars 1971 Unique Structural Analysis and Tests*, Rept. 610-176, March 26, 1971, Jet Propulsion Lab., Pasadena, Calif.

[19] Trubert, M. R., *A Fourier Transform Technique for the Prediction of Torsional Transients for a Spacecraft from Flight Data of Another Spacecraft Using the Same Booster*, TM 33-350, Oct. 15, 1967, Jet Propulsion Lab., Pasadena, Calif.